

# Multimodal Biometric System Using Face-Iris Fusion Feature

Zhifang Wang, Erfu Wang, Shuangshuang Wang and Qun Ding

Key Laboratory of Electronics Engineering, College of Heilongjiang Province,

School of Electronic Engineering, Heilongjiang University, Harbin, China

Email: zhifang.w@gmail.com, efwang\_612@163.com, 278705905@qq.com, qunding@yahoo.cn,

**Abstract**—With the wide application, the performance of unimodal biometrics systems has to contend with a variety of problems such as background noise, signal noise and distortion, and environment or device variations. Therefore, multimodal biometric systems are proposed to solve the above mentioned problems. This paper proposed a novel multimodal biometric system using face-iris fusion feature. Face feature and iris feature are first extracted respectively and fused in feature-level. However, existing feature level schemes such as sum rule and weighted sum rule are inefficient in complicated condition. In this paper, we adopt an efficient feature-level fusion scheme for iris and face in series. The algorithm normalizes the original features of iris and face using z-score model to eliminate the unbalance in the order of magnitude and the distribution between two different kinds of feature vectors, and then connect the normalized feature vectors in serial rule. The proposed algorithm is tested using CASIA iris database and two face databases (ORL database and Yale database). Experimental results show the effectiveness of the proposed algorithm.

**Index Terms**—feature fusion, multimodal biometrics, unimodal biometrics

## I. INTRODUCTION

A wide variety of applications require reliable verification schemes to confirm the identity of an individual. The systems in the absence of robust verification schemes are vulnerable to the attack of an impostor. Traditionally, passwords (knowledge-based security) and ID cards (token-based security) have been used to restrict access to applications. However, security would be lost when password or ID cards is revealed or stolen in these applications. The emergence of biometrics has solved the above problems. Biometrics refers to the automatic identification (or verification) of an individual (or a claimed identity) by using certain physiological or behavioral traits associated with the person.

Biometrics has drawn extensive attention during the past decades for its huge potentials in many applications. However, the performance of unimodal biometrics systems has to contend with a variety of problems such as background noise, signal noise and distortion, and environment or device variations [1]. Therefore, multimodal biometric systems are proposed to solve the above mentioned problems. Many literatures and algorithms are presented to do research about multimodal

biometric fusion [2-4].

Based on the occurred phase of fusion in the biometric system, there are various levels of fusion for combining two (or more) biometric systems. The initial approach is the decision level [5-6]. In this scheme, each sensor can individually capture multiple biometric data and the resulting feature vectors which classified into the two classes—accept or reject. Finally, a majority vote scheme can be used to make the final decision. On the other hand, matching score level is the popular approach [7-8]. Each system provides a matching score to estimate the similarity of the feature vector with the template vector. These scores can be combined to analyses synthetically the veracity of the claimed identity.

Along with the fusion in matching score level and decision level, one important branch is to perform fusion in feature level which can derive the most discriminative information from original multiple features sets and eliminate the redundant information resulting from the correlation between different feature sets. The data obtained from each sensor is used to compute a feature vector. Two vectors are concatenated into a single new vector. The new feature vector now represents a person's identity in a different data space. In general, there is a basic mode for feature level fusion: weighted sum rule [3-5], which means sum the weighted corresponding dimension of two different vectors. Nevertheless, how to select the weighted value is a contentious issue. Comparing with this parallel fusion rule, we fuse the two feature sets in series. Human iris provides unique, rich and stable texture suitable for non-invasive biometric assessment. Comparing with other kinds of biometrics, such as fingerprint, face, palm, voice and so on, iris recognition system has some key advantages in terms of speed, simplicity, accuracy and applicability. In addition, face recognition is more friendly and non-invasive than other biometrics. Then we are motivated to design a face-iris recognition algorithm in feature level fusion.

The rest of this paper is organized as follows: In the next section, we present feature extraction of face and iris. Section 3 normalizes face feature and iris feature, and performs fusion and classification. In section 4, experimental results and comparison are given. Finally, we conclude in section 5.

## II. FEATURE EXTRACTION

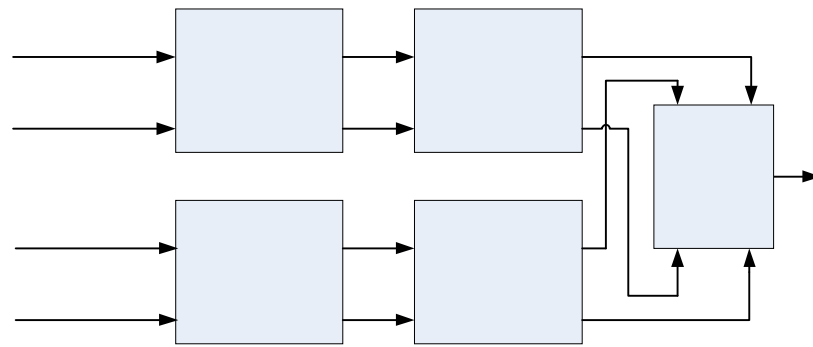


Figure 1 The framework of the proposed algorithm

The composition of a multimodal biometric system is similar with an unimodal biometric system. Furthermore, we classify fusion level according to the fusion stage in the whole biometric system. So this section first introduces the composition of a biometric system. In generally, a simple biometric system includes four important components:

- Sensor module acquires the biometric data of an individual. An example is a face sensor that captures face images of a user.
- Feature extraction module processes the acquired data to extract feature values. For example, the position and orientation of the texture in an iris image would be extracted in the feature extraction module of a iris system.
- Matching module compares the feature values against the template vector by generating a matching score. For example, in this module, the distance of two matching feature vectors will be computed and treated as a matching score.
- Decision-making module claims the user's identity: accepted or rejected based on the matching score generated in the matching module.

Then, we present the framework of the multimodal biometric algorithm as Fig. 1. The algorithm comprises 3 phases. In the first phase, the features of iris and face are extracted respectively. We then normalize the features before fusion. Finally, we fuse the normalized features in series and use Euclidean distance to classify. The following content will describe feature extraction. In this algorithm, the objects for fusion are iris features and face features. So the first step is to obtain them. This section describes the feature extraction of iris and face respectively.

A. Face feature extraction

As one of the biometric technologies that possess the merits of both high convenience and low intrusiveness, face recognition has the wide application fields such as information security, law enforcement and surveillance, smart cards, access control. As a result, numerous face recognition algorithms and surveys have been presented [9-14]. One of the popular approaches for face recognition is eigenface method (Principal Component Analysis, PCA) [15]. The key idea is to find the best set of projection directions to span the feature space that will maximize the total scatter.

More formally, we suppose there are  $n$  known pattern classes  $\{X_i | i = 1, 2, \dots, n\}$ , and each element in the set of training sample images  $\{x_j^i | i = 1, 2, \dots, n, j = 1, 2, \dots, m\}$  belongs to one of  $n$  classes, taking values in an  $d$ -dimensional image space. Given a projection matrix with orthonormal columns  $W_{PCA}$ , which maps the original image space into the feature space, the new projected feature vectors  $y_j^i$  of the  $j$ th training sample  $x_j^i$  from the  $i$ th class is defined by the following linear transformation

$$y_j^i = W_{PCA}^T x_j^i \tag{1}$$

In this phase, PCA selects projection  $W_{PCA}$  to maximize the total scatter matrix  $S_T$ , which is defined as

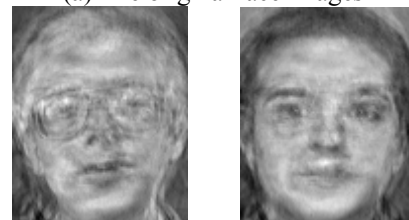
$$S_T = \sum_{i=1}^n \sum_{j=1}^m (x_j^i - \bar{x})(x_j^i - \bar{x})^T \tag{2}$$

where  $\bar{x} = \frac{1}{nm} \sum_{i=1}^n \sum_{j=1}^m x_j^i$  is the mean image of all training sample images. The optimal projection  $W_{PCA}$  is computed by the following objective function

The corresponding eigenfaces of the image



(a) The original face images



(b) The eigenface of (a)

Figure 2 The corresponding eigenfaces of the image

$$W_{PCA} = \arg \max_W |W^T S_T W| \tag{3}$$

$$= [u_1 u_2 \dots u_m]$$

Here the columns of  $W_{PCA}$  are the eigenvectors of  $S_T$  corresponding to the  $m$  largest eigenvalues. The above method can be briefly described as follows:

- Transform the matrixes of the face images into the vectors as the training samples;
- Compute the mean image of all training sample  $\bar{x}$  ;
- Construct total scatter matrix  $S_T$  as (2);
- Calculate the eigenvalues and the corresponding eigenvectors of  $S_T$  , and all eigenvectors compose the projection matrix  $W_{PCA}$  ;
- Compute the projected feature vectors  $y_j^i$  as (1);
- Calculate the Euclidean distance between the projected feature vectors and the template vectors and do the classification.

The reason for this approach to be called eigenface method is because the projected feature vectors can construct a face with most eigen information of the individual. Fig. 2 shows the examples of the eigenface.

*B. Iris feature extraction*

For iris recognition, Gabor filter is the popular feature extractor. For example, Daugman [17] takes 2D Gabor filter while Tan [18] uses 2D even Gabor filter. However, the feature attained by Daugman’s method is not convenient for fusion with face feature, which is represented as binary vector. Therefore, this algorithm adopts the latter method and obtains the iris feature represented as the real vector.

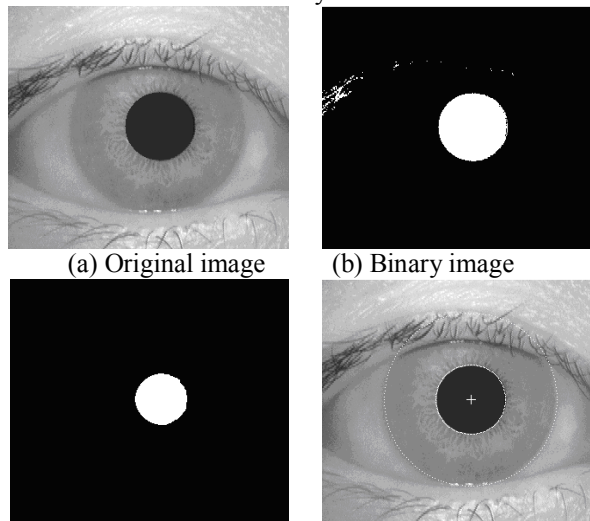
In generally, an iris image contains not only the iris, but also data attained from the surrounding eye region. Only the portion of iris derived from outside the pupil and inside the sclera without the eyelids should be included. The accuracy of iris location will influence the performance of the whole system. Therefore, before the later processes such as feature extraction, the iris location is a key step.

The iris is an annular part between the pupil and the sclera. Therefore, before iris feature extraction, it is important to locate the iris. In other words, two borders should be confirmed, which are the inner boundary (the border between the pupil and the iris) and the outer boundary (the border between the iris and the sclera). From an iris image, such as fig.3(a), it can be found that the gray level is increasing from the inner to the outer among three portions: the pupil, the iris and the sclera. This characteristic can be taken to locate the inner boundary and the outer boundary.

In order to confirm the center and radius of pupil, we get the binaryzation image by adaptively selecting a reasonable threshold. Both the inner boundary and the outer boundary can approximately be regarded as a circular contour. In the binary image, such as fig.2 (b), some eyelashes are left besides pupil. For the purpose of

eliminating the effect of eyelashes, an open operator is adopted. The result is shown as fig.2(c). After the processing, the center  $(x_0, y_0)$  and inner radius  $r$  can be gotten.

In the reference [17], an integrodifferential operator is presented to locate the boundary:



(c) The result of open operator (d) The result of location  
Figure 3 The processing of iris boundaries location

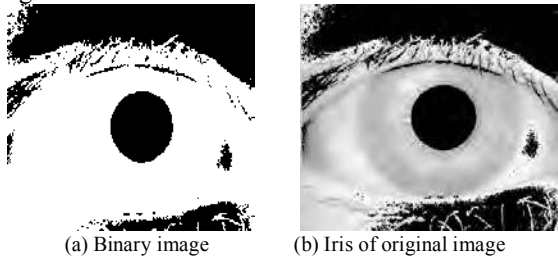
$$\max_{(r, x_0, y_0)} |G_\sigma(r) * \frac{\partial}{\partial r} \oint_{r, x_0, y_0} \frac{I(x, y)}{2\pi r} ds| \tag{4}$$

Where  $r, x_0, y_0$  denote radius and the coordinate of the pupil center respectively.  $I(x, y)$  is an iris image such as fig.2(a).  $G_\sigma(r)$  represents a Gauss filter. The essential purpose of the operator is to search the circle with the maximum of the contour integral as radius  $r$  increases. This section improves the method at the following points:

1. Searching area: The whole iris image is taken as searching area in [17]. In this way, the time cost of searching will be expensive. In addition, occluding of eyelids will cause deviation from the outer boundary. So we choose the range with the angle  $[-\frac{\pi}{12}, \frac{\pi}{12}]$  and  $[\frac{11\pi}{12}, \frac{13\pi}{12}]$  in the polar coordinate same as [17], in which the influence of eyelids and eyelashes can almost be avoided.
2. Best step length: In order to accelerate the searching speed and decrease searching times, the best step length is calculated. If  $I$  and  $X$  represent the searching radius and step length respectively, the searching times will be  $\frac{I}{X} + X$  . Based on inequality  $a + b > 2\sqrt{ab}$  , we can get the minimum searching times  $2\sqrt{I}$  . At the same time, the best step length is  $\sqrt{I}$  .

After the process, the inner boundary and outer boundary can be rapid and valid located as shown in fig.3 (d).In iris image, eyelashes distribute unorderedly and always occlude the edge between eyelids and iris. We

solves this problem by using Gabor filter and weight filter. Because the following steps are all operated in the portion of iris, we should select a reasonable threshold to binary the image and extract the part of iris. Then the same part of original image can be gotten by inner product of the binary image and the original image. The result is shown in fig. 4.



(a) Binary image (b) Iris of original image  
Figure 4 The preprocessing of iris image

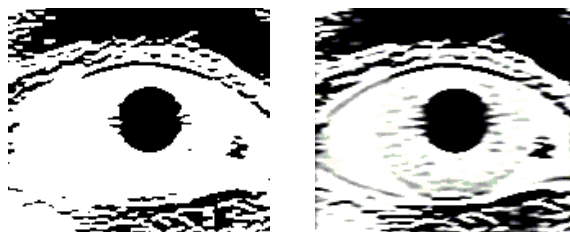
### 1. 2D Gabor filter

The 2D Gabor functions proposed by Daugman are local spatial bandpass filters. The reference [17] describes a method to extract the feature by taking advantage of 2D Gabor filter. This paper selects 2D Gabor filter with a special angle to eliminate the influence of eyelashes. Fig.5 (a) shows the result.

### 2. Weighted Filter

From fig.5 (a), we can find that the texture almost trend towards horizontal direction. But it is not enough continuous to represent the integrality of eyelids. In order to improve the continuity of texture and prepare for the subsequent algorithm, weight filter is used to increase the effect of horizontal direction. Experiments show that the following filter mask  $h$  with size  $3 \times 11$  can get the finer result, shown in fig.5 (b).

$$h = \begin{bmatrix} 2 & 2 & 2 & 2 & 0 & 0 & 0 & 2 & 2 & 2 & 2 \\ 3 & 3 & 3 & 3 & 1 & 1 & 1 & 3 & 3 & 3 & 3 \\ 2 & 2 & 2 & 2 & 0 & 0 & 0 & 2 & 2 & 2 & 2 \end{bmatrix}$$



(a) Gabor filtered image (b) Weighted filtered image  
Figure 5 The filtering preprocessing of iris image

In normal condition, the eyelids always cover the iris especially the upper eyelid. If the occluded part of the iris takes part in feature extraction, the accuracy of the whole system will be influenced. So prior to feature extraction, it is necessary to locate the eyelids and mark the occluded part of the iris. However, few of literatures describe this problem. In this section, we propose two eyelid location methods: the ridge-tracing method and the radius-differential method, and give the comparison result of two methods.

### 1. Ridge-tracing Method

In fingerprint recognition, the method of ridge-tracing is applied widely [20, 21]. This paper utilizes the idea to trace the edges of eyelids. Firstly, canny operator is used to detect the skeleton of the filtered image. Fig.6 shows that the trend of the edges approximately parallels to the horizontal direction. The following content describes the method in detailed:



Figure 6 The result of canny operator

- Select start-point: The accuracy of start-point location influences the performance of the algorithm. And the site of start-point affects the calculation consuming. The searching area  $A$  is provided as follows:

$$A = \{(\rho, \theta) \mid \rho \in [\bar{r}, R], \theta \in [\frac{\pi}{4}, \frac{3\pi}{4}]\}$$

- From the central section of  $A$ , search the first point with non-zero value as polar angle  $\theta$  decreasing between the inner radius  $r$  and the outer radius  $R$ . This point is regarded as the start-point of the upper eyelid provisionally. The method of searching start-point in the lower eyelid is the same as the upper eyelid.
- Estimate the continuity of start-point: If there is one or more points with non-zero value among three points in next column of start-point, it is considered to be continuous. Otherwise, it is discontinuous. Then go back to the first step.
- Measure the continuity of ridge: Based on the rule of the second step, trace the ridge and calculate the length of the ridge until there is none point with non-zero value. If the length is greater than or equal to  $1.5R$  and the angle of the beeline connecting start-point and end-point is not larger than  $\frac{\pi}{6}$ , the ridge is regarded as continuous. Otherwise go back to the first step.

After all the steps, we can get the eyelids by fitting quadratic curve using the points in the ridge. The result is shown in fig.7 (a).

### 2. Radius-differential Method

Daugman's integrodifferential operator searches the circle with the maximum of the contour integral with respect to increasing the searching radius. In generally, the iris is darker than the eyelids. This paper takes advantage of the characteristic to fix on eyelids based on integrodifferential operator. The method is described as follows:

1. Predigest the searching function: Predigest the integral curve to one pixel and search the pixel with the maximum change of gray value according to the following searching function:

$$\max_r |I(x, y)|$$

2. Judge whether or not the eyelid cover iris: Along the

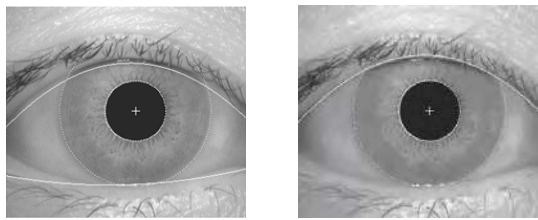
polar axis with the angle  $\frac{\pi}{2}$ , search the pixel satisfying the above function and calculate the distance from the point to the center of pupil. By comparing the distance with outer radius  $R$ , if the distance is less than  $R$ , we can conclude iris is occluded by eyelids and do the following steps. Otherwise, quit the process of eyelids location.

3. Define the searching area: Search the points meeting the conditions:

$$A = \{(\rho, \theta) \mid \rho \in [\bar{r}, R], \theta \in [\frac{\pi}{4}, \frac{3\pi}{4}]\}$$

4. Fit the eyelid: Fit all points attained from the above steps into the quadratic curve. Then we can get upper eyelid.

Lower eyelid can be located by the same process of upper eyelid. The result is shown in fig.7 (b).



(a) Ridge-tracing method (b) Radius-differential method  
Figure 7 The result of eyelids location

After preprocessing, we can segment the portion of the iris. And then we extract the feature from the iris using 2D even Gabor filter. Gabor function possesses the fine characteristic in direction and frequency. A self-similar multichannel filter family is obtained by rotation, scaling and translation of the Gabor function. 2D even Gabor filter is defined as follows:

$$g(x, y) = \frac{1}{2\pi\sigma_x\sigma_y} \exp[-\frac{1}{2}(\frac{x^2}{\sigma_x^2} + \frac{y^2}{\sigma_y^2})] \cdot \cos(2\pi f\sqrt{x^2 + y^2}) \quad (5)$$

where  $\sigma_x, \sigma_y$  are the parameter of scale,  $f$  denotes the frequency. We divide the segmented iris image into sub-image with the same size, and respectively filter them using the Gabor filter family. The  $j$ th filtered sub-image is attained by

$$F_j(m, n) = \iint I(x, y) g_i(m-x, n-y) dx dy \quad (6)$$

Where  $g_i(x, y)$  is  $i$ th even Gabor filter. Finally, the absolute mean deviation is defined as the iris feature of the  $j$ th filtered sum-image

$$V_j = \frac{1}{N} (\sum_N F_j(m, n) - M) \quad (7)$$

where  $M$  denotes the mean value of the filtered sub-image, and  $N$  is the number of the filtered sub-image. All the absolute mean deviation of the filtered sub-image composed the iris feature.

Whereas the dimension of iris features derived by Tan's method is too large, PCA are used to solve this problem and control the dimension of iris feature equal to that of face feature.

### III. NORMALIZATION AND FEATURE FUSION

#### A. Normalization

Traditionally, feature-level fusion methods directly fuse two kinds of features after feature extraction. As we know, due to the difference of the modal and extraction method, the order of magnitude and the distribution between iris feature and face feature might be different. In order to eliminate the unbalance and get good performance, we are motivated to normalize the feature before fusion using z-score model.

Let  $a_j^i$  be a  $d$ -dimension iris feature of the  $j$ th iris training sample from the  $i$ th class, and  $b_j^i$  denotes a  $d$ -dimension face feature of the  $j$ th face training sample from the  $i$ th class. Then the iris feature set and the face feature set are respectively represented as  $A = (a_1^1, \dots, a_m^1, a_1^2, \dots, a_m^n)$  and  $B = (b_1^1, \dots, b_m^1, b_1^2, \dots, b_m^n)$ .

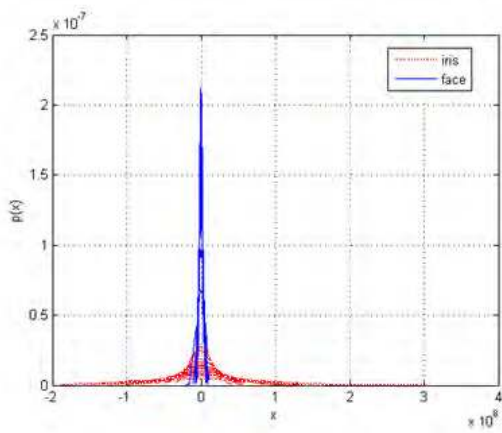
Let  $A_k$  is the  $k$ th row of the iris feature set  $A$ . We use the following method to get the corresponding normalized component  $X_k$ . Firstly, compute

$$C_k = \frac{A_k - \bar{A}_k}{\sigma_k} \quad (8)$$

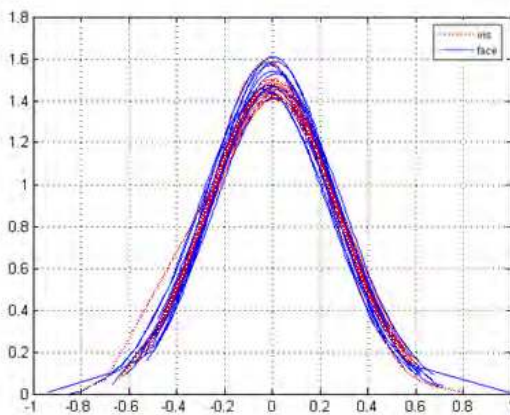
where  $\bar{A}_k$  denotes the mean value of  $A_k$ , and  $\sigma_k$  is the standard deviation of  $A_k$ . Then, we can get the normalized component by

$$X_k = \frac{C_k - C_{\min}}{C_{\max}} \quad (9)$$

where  $C_{\min}$  and  $C_{\max}$  denote the minimum value and the maximum value of  $C_k$  respectively. The normalized feature set is  $X = (X_1, \dots, X_d)$ . For face feature, repeat the same procedure and get the normalized feature set  $Y = (Y_1, \dots, Y_d)$ . Fig. 8(a) gives the distribution of the original components. After the normalization, the distribution is changed as fig. 8 (b). From them, it can be found that the order of magnitude and the distribution of two kinds of features are similar after normalization.



(a) The original components



(b) The normalized components  
Figure 8 The distribution of the components

**B. Feature Fusion**

Let  $X = (x_1, \dots, x_d)$  denotes a normalized iris feature vector,  $Y = (y_1, \dots, y_d)$  is a normalized face feature vector. The fusion feature  $\xi$  in sum rule can be defined as  $\xi = (x_1 + y_1, \dots, x_d + y_d)$ . For weighted sum rule, we take  $\theta = 3/7$  as the weighted parameter because the performance of iris recognition is better than that of face recognition. The fusion feature in weighted sum rule can be denoted as  $\xi = (x_1 + \theta y_1, \dots, x_d + \theta y_d)$ . So, sum rule can also be considered as the special case of weighted sum rule. In this paper, we adopt the series fusion method. The format of the fusion feature is defined as  $\xi = (x_1, \dots, x_d, y_1, \dots, y_d)$ . This method combines two kinds of feature into a long vector. Then Euclidean distance is selected to classify the fusion features.

**IV. EXPERIMENT**

The experiments are performed on CASIA iris image database (ver. 1.0) and two face databases: ORL database and Yale database. Our goal is to compare our algorithm with two unimodal biometrics (face [17] and iris [18]).

And sum rule can be taken as a special case of weighted sum rule to experiment.

**A. Database**

The experiments were performed on CASIA iris image database (ver.1.0) and two face databases (ORL database and Yale database). CASIA iris image database (ver. 1.0) includes 756 iris images from 108 eyes (hence 108 classes). Fig. 9 gives some iris images in this database. For each eye, 7 images are captured in two sessions, where three samples are collected in the first session and four in the second session. Other samples are used to test the performance of the algorithm. ORL face database is used in this paper. It includes 40 people, 10 different images with pose and expression variation per person. Yale face database contains 11 images of 15 people in a variety of conditions including with and without glasses, illumination variation, and changes in facial expression. Fig. 10 and fig. 11 give some face images in these two databases.

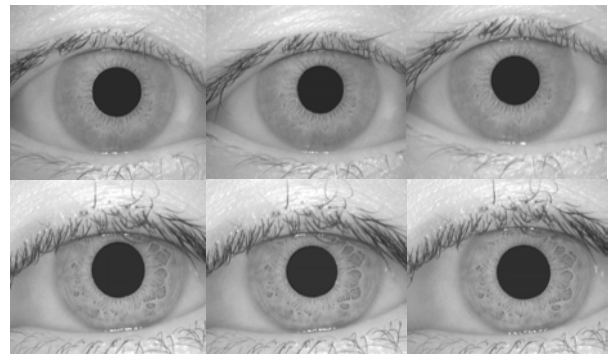


Figure 9 The iris image in CASIA database

Two experiments were conducted: Experiment I fuses CASIA iris features with ORL face features; Experiment II fuses CASIA iris features with Yale face features. In order to fuse the different features derived from iris and face, the dimension and the number of the feature should be equal. The former problem has been solved in the



Figure 10 The face image in ORL database

process of the feature fusion. Aim to the latter, this paper adopts the following rule: according to the number of the sample in the face database, we randomly select the same number of the iris sample. Taking experiment I as an example, because ORL face database includes 40 people, we choose 40 eyes of CASIA database at random

TABLE I  
EER OF TWO EXPERIMENTS

Method	Face	Iris	Sum rule	Weighted rule	Series rule
Experiment I (EER %)	7.79	3.11	4.22	2.5	1.94
Experiment II (EER %)	28.33	3.33	9.63	5.54	1.67

to fuse. And the previous 7 images per person of ORL database are used. 3 images per person are selected as the training samples, the remainder images are taken as the testing set.



Figure 11 The face image in Yale database

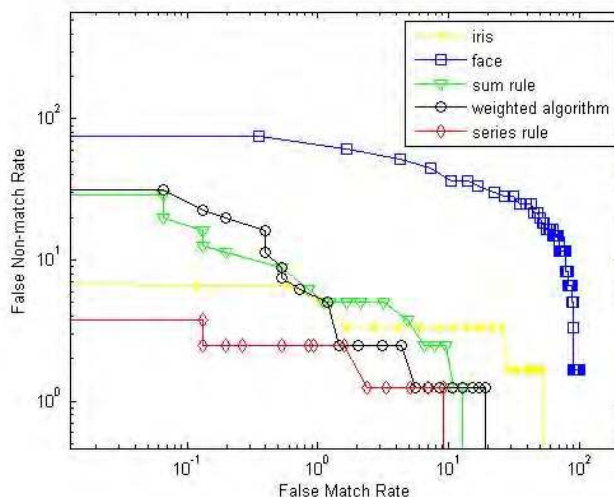
**B. Experimental Results**

False reject rate (FRR) and false accept rate (FAR) are usually used to test the performance of the system. However, False match rate(FMR) and false non-match rate(FNMR) are more suitable to evaluate the performance of the algorithms in an off-line technology test like this as failure to enroll rate(FTE) and failure to acquire rate(FTA) are not available [19]. Thus, FMR and FNMR are used as the performance parameters of the proposed algorithm in this paper. Equal error rate (EER) is also taken as a performance parameter.

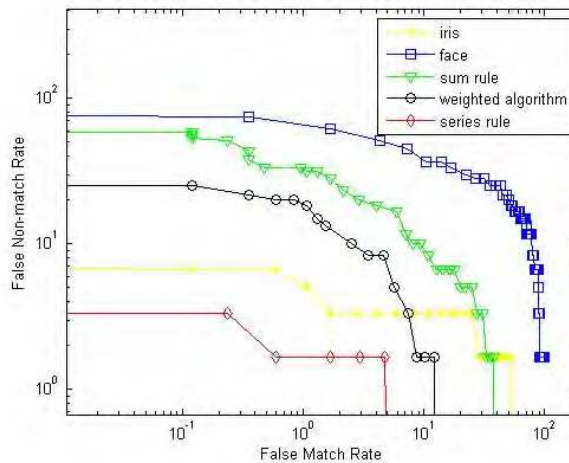
Table1 is evident that EER of unimodal biometrics is efficiently reduced after series rule in proposed method. Comparing with other two fusion approaches, our algorithm is still better. In order to present the whole performance of proposed algorithm, we give the DET curves of five algorithms as fig. 12. Compared with sum rule and weighted sum rule, series rule can be also considered as a feature connector to fuse discriminative information of two kinds of biometric feature. From fig. 12, it indicates that our algorithm has much efficiency than other algorithms.

**V. CONCLUSION**

In this paper, a multimodal biometric algorithm for iris and face is proposed. The algorithm first extract face feature based on eigenface method and iris feature using 2D even Gabor filter, and then adopts z-score normalization model to eliminate the difference of the



(a) Experiment I



(b) Experiment II

Figure.12 DET curves of two experiments

order of magnitude and the distribution between iris features and face features. The normalized features are combined in series and take Euclidean distance as a classifier. We perform experiments on CASIA iris database and two face database (ORL database and Yale database). Experiments show that our algorithm improves the performance of two unimodal biometrics and outperforms sum rule fusion and weighted sum rule fusion.

## ACKNOWLEDGMENT

This work is supported by the National Science Foundation of China (no.60672011), Open Fund of Key Laboratory of Electronics Engineering, College of Heilongjiang Province, and Startup Fund for Doctor of Heilongjiang University.

## REFERENCES

- [1] M. Khan and J. Zhang. Multimodal face and fingerprint biometrics authentication on space-limited token. *Neurocomputing*, vol. 71, pp. 3026–3031, 2008.
- [2] K. Jain and A. Ross. Multibiometric systems. *Communications of the ACM*, vol. 47, pp. 34–40, 2004.
- [3] J. Kittler, M. Hatef, R. Duin, and J. Matas. On combining classifiers. *IEEE Transaction on Pattern Analysis and Machine Intelligence*, vol. 20, pp. 226–239, 1998.
- [4] Ross and A. Jain. Information fusion in biometrics. *Pattern Recognition Letters*, vol. 24, pp. 2115–2125, 2003.
- [5] S. Prabhakar and A. Jain. Decision-level fusion in fingerprint verification. *Pattern Recognition*, vol. 35, pp. 861–874, 2002.
- [6] J. Fierrez-Aguilar, D. Garcia-Romero, J. Ortega-Garcia and J. Gonzalez-Rodriguez. Adapted user-dependent multimodal biometric authentication exploiting general information. *Pattern Recognition Letter*, vol. 26, pp. 2628–2639, 2005.
- [7] A. Rajagopalan, K. Rao and Y. Kumar. Face recognition using multiple facial features. *Pattern Recognition Letter*, vol. 28, pp. 335–341, 2007.
- [8] K. Toh, J. Kim and S. Lee. Biometric scores fusion based on total error rate minimization. *Pattern Recognition*, vol. 41, pp. 1066–1082, 2008.
- [9] Q. Sun, S. Zeng, Y. Liu, P. Heng, and D. Xia. A new method of feature fusion and it application in image recognition. *Pattern Recognition*, vol. 38, pp. 2437–2448, 2005.
- [10] R. Chellappa, C. L. Wilson, and S. Sirohey. Human and machine recognition of faces: A survey. *Proceedings of IEEE*, vol. 83, pp. 705–740, May 1995.
- [11] J. Daugman. Face and gesture recognition: Overview. *IEEE Transaction on Pattern Analysis and Machine Intelligence*, vol. 19, pp. 675–676, July 1997.
- [12] W. Zhao, R. Chellappa, P. J. Phillips and A. Rosenfeld. Face recognition: A literature survey. *ACM Computing Surveys*, pp. 399–458, December 2003.
- [13] A. Samal and P. A. Iyengar. Automatic recognition and analysis of human faces and facial expressions: A survey. *Pattern Recognition*, vol. 25, pp. 65–77, 1992.
- [14] D. Valentin, H. Abdi, A. J. O’Toole, and G. W. Cottrell. Connectionist models of face processing: A survey. *Pattern Recognition*, vol. 27, pp. 1208–1230, 1994.
- [15] M. Turk, A. Pentland. Face Recognition Using Eigenfaces. In: *Proc. IEEE Computer Vision and Pattern Recognition*, pp. 586–591, 1991.
- [16] J. Daugman. How Iris Recognition Work. *IEEE*

*Transaction on Circuits and Systems for Video Technology*, vol. 14, pp. 21–30, 2004.

- [17] L. Ma, T. Tan, Y. Wang and D. Zhang. Personal Identification Based on Iris Texture Analysis. *IEEE Transaction on Pattern Analysis and Machine Intelligence*, vol. 25, pp. 1519 – 1533, 2003.
- [18] ISO/IEC 19795-1:2006 Information technology - Biometric Performance Testing and Reporting - Part 1: Principles and Framework
- [19] X. Jiang, W. Yau and W. Ser. Detecting the fingerprint minutiae by adaptive tracing the gray level ridge. *Pattern Recognition*, vol. 34, pp. 999–1013, 2001.
- [20] Q. Zhang and H. Yan. Fingerprint classification based on extraction and analysis of singularities and pseudo ridges. *Pattern Recognition*, vol. 37, pp. 2233–2243, 2004.



**Zhifang Wang** Henan province, China, 1979. Received PhD degree and M.S. degree in Harbin Institute of Technology, China, in 2009 and 2005 respectively, and B.S. degree in Henan University, China. The interest fields are biometric, development of media systems, image analysis, cluster analysis, etc. Currently, she is a lecturer of Heilongjiang University, China.



**Erfu Wang** Heilongjiang province, China, 1980. Received PhD degree and M.S. degree in Harbin Institute of Technology, China, in 2009 and 2005 respectively, and B.S. degree in Jilin University, China. The interest fields are blind source separation, array signal processing, wideband wireless communication, etc.



**Qun Ding** Heilongjiang province, China, 1957. Received PhD degree and M.S. degree in Harbin Institute of Technology, China, in 2007 and 1997 respectively. The interest fields are secure communication, information security, Pattern recognition, etc. Currently, she is a professor of Heilongjiang University, China.



**Shuangshuang Wang** Heilongjiang province, China, 1984. Received B.S. degree in Heilongjiang University, China, in 2008. The fields of research are image processing, pattern recognition, etc